Amplification Enhancement of Gunn Effect Based Active Transmission Lines

M. Pokorný, Z. Raida
Department of Radio Electronics, Brno University of Technology
Purkyňova 118
Brno, Czech Republic

***Abstract* - In this paper, we concentrate on the design and analysis of the active semiconductor traveling wave devices based on the Gunn effect in bulk GaAs semiconductor. The complex model of active device based on the macroscopic approximations of electron dynamics is analyzed by finite element method using COMSOL Multiphysics and the design issues to achieve an efficient amplification and device stability are formulated and discussed. Upon simulation results of the convectional active coplanar waveguide design based on the experimental work in [1], we propose more efficient solution.**

I. Introduction

Since the active semiconductor devices are limited by the transit time of charge carriers or high field domains through the structure, the miniaturization is the key to achieve the operation at high frequencies (at sub-millimeter and millimeter wavelengths). However, reduced device dimensions make it difficult to effectively dissipate a heat and together with reduced device efficiency led to the crucial limitation in the output power [2]. Furthermore, the miniaturized transmission lines that connect the active devices with electronic circuits and systems suffer by extreme attenuation at millimeter wave band [3].

One possible solution to overcome such fundamental limitations is to leave the concept of the lumped active components and focus on the devices based on distributed parameters [2]. Beside the approaches as the multi-element network and power combiners, two basic types of semiconductor distributed amplifying structures, which differ by orientation of the wave-vector **k** relative to the drift velocity of carriers **v**, are in the scope of interest. Proximity of the phase velocity of the wave to the carrier drift velocity is the characteristic property for structures with parallel drift where $\mathbf{v} \parallel \mathbf{k}$. In structures with transversal drift, when $\mathbf{v} \perp \mathbf{k}$, the waves propagate with velocity close to the speed of light in the medium and the effect of amplification occurs due to coincidence of the transverse components of the electric field with the transverse drift of carriers in a semiconductor [4].

In this paper, we focused on the active devices based on the transversal drift interaction in GaAs semiconductors which is characterized with the bulk negative differential conductivity (BNDC). Up to date, there are mainly experimentally oriented results in this field. The first successful experiments on electromagnetic wave amplification by BNDC is based on the coplanar waveguide design on GaAs wafer at frequency about 20 GHz [1]. Other experiments dealt with a fin-line inside the rectangular waveguide at the frequencies about 40 GHz [2]. All published works are based on the devices using the coplanar configuration of the voltage terminals.

This work is focused on the improvement of such BNDC based devices, particularly on the achievement of the higher gain and the higher operating frequency. The paper is organized as follows. Section II briefly discusses the issue of the device-level simulation and describes the macroscopic approximation of the Gunn effect and the evaluation of the device stability. The section III presents the results of the complex numerical calculations of the convectional design represented by the active coplanar waveguide and describes the principle of device performance improvement. The section IV compares the numerical results of the transmission properties and Section V concludes the paper.

II. Modeling of the Gunn Effect Based Devices

The device characterization cannot be restricted to the analysis of the active region only. The supporting materials, metal contacts and other interfaces have a significant effect on the device performance, so the whole device should by included in the simulation. The device level modeling of the semiconductor devices at microwave frequencies is facing to the problems of the enormous complexity and computational demands of the full-wave formulation of the coupled wave-transport phenomena. A very general formulation of such coupled problem has been proposed in [5]. However it results in computational complexity which practically limits the analysis to a 1D cross section.

Our approach is based on the use of the macroscopic approximations of the electron physics for the characterization of the semiconductor media properties in the small-signal approximation. This way we can use the semi-classical approaches for the semiconductor devices simulation.

The carriers transport phenomena is modeled by thermodynamic drift-diffusion scheme (TDD) which represents the trade-off between complexity and the accuracy of the device-level simulations of semiconductor structures [6], [7].

Inclusion of the Gunn effect in the scheme at the microscopic scale requires the calculation of the hot electrons transfer from central valley Γ to the upper valleys X and L of

conduction band in momentum space. Such calculation for the bulk GaAs using Monte Carlo method was published in [8] and the result was generalized in the model of the macroscopic field dependent electron mobility. We use this model in the thermodynamic drift-diffusion computations and for the purpose of the high-frequency calculations in small-signal approximation we derive its differential form as

$$\mu_n^D = v_{sat}^L \left(\frac{1}{E_{crit}\left(A\left(E_0/E_{crit}\right)^g + 1\right)} - \frac{Ag\left(E_0/E_{crit}\right)^{g-1}\left(E_0/E_{crit} - 1\right)}{E_{crit}\left(A\left(E_0/E_{crit}\right)^g + 1\right)^2} \right), \qquad (1)$$

where v_{sat}^L is the temperature dependent electron saturation velocity, E_{crit} is the threshold electric field, A and g are the approximation coefficients whose expressions can be found in [8]. While the bulk GaAs sample is assumed to be biased by electrostatic field $\mathbf{E}_0$, the E_0 denotes the component of $\mathbf{E}_0$ in the direction of the electron current density vector $\mathbf{J}_n$, which can be evaluated as

$$E_0 = \frac{\mathbf{E}_0 \cdot \mathbf{J}_n}{\left|\mathbf{J}_n\right|}. \qquad (2)$$

That follows that the mobility μ_n^D have to be represented as the uniaxial tensor due to anisotropy character of the Gunn effect resulting from (2).

In the calculation [8] and consequently in the equation (1) is assumed the static or very slow variation of the electric field. However, at high frequencies the velocity and diffusion of electrons do not instantaneously follow the variations of the electric field and the mobility becomes frequency dependent. Using the precise Monte Carlo calculations of the electron mobility properties in GaAs at microwave frequencies published in [9] we formulate the frequency and temperature dependent correction term to the static electron differential mobility (1). The final expression is

$$\mu_n^{DF} = \mu_n^D + \frac{a_1}{T} e^{-\left(\frac{(E_0 - b_1)}{c_1}\right)^2} + \frac{a_2}{T} e^{-\left(\frac{(E_0 - b_2)}{c2}\right)^2}, \qquad (3)$$

where T is the temperature and the coefficients $a_{1,2}$, $b_{1,2}$, $c_{1,2}$ are given by polynomials of first and second order whose can be found in [10]. The evaluated characteristics of the μ_n^{DF} are depicted in the Fig. 1 for the various frequencies and temperatures. The crosses denote the numerical results taken from [9].

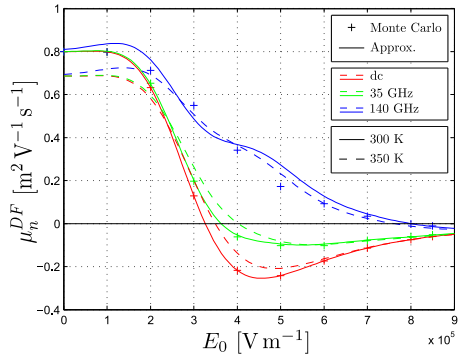

Figure 1. Frequency and temperature dependent differential mobility characteristics.

It is well known that the moving space-charge instabilities (Gunn domains) can be formed in the bulk GaAs semiconductor in the high intensity electric field. They can be observed as the short current pulses at terminals with frequency given by transit time between the device terminals. This self-oscillation behavior is highly undesirable for the purpose of the stable amplification. If we ensure that the domain formation time is greater than the domain transit time, the domain does not have enough time to develop and the sample is stable. This condition can be derived using equivalent R-C circuit [8], [10] as

$$LN_D^+ < \frac{\varepsilon v_{sat}^L}{q\left|\mu_n^D\right|}, \qquad (4)$$

where L represents the device length (voltage terminal distance), N_D^+ is the doping concentration by donors, ε is the permittivity and q is the elementary charge. For the homogenous GaAs sample the criterion (4) can be evaluated as

$$LN_D^+ < 1\times10^{15}\,\mathrm{m}^{-2}. \qquad (5)$$

III. Design and Calculation Results

The concept of the active BNDC based travelling wave transmission line was successfully verified by experiments in continuous and pulse regime [1]. Further we have focused only on the continuous regime, because it represents the worst case in terms of heat dissipation.

We have developed the cross-section model of the 50 Ω active coplanar waveguide (ACPW) on the low n-doped GaAs substrate with thickness of 300 μm according to the Fig. 2.

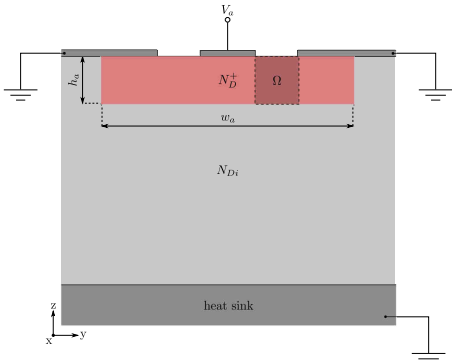

Figure 2. Active coplanar waveguide structure.

Due to the coplanar configuration of voltage terminals, the steady current $\mathbf{J}_n$ is expected to flow dominantly along the surface in parallel to the transversal electric components of the propagating fundamental mode field $\mathbf{E}_p$. It follows that the highly n-doped area (active region) should located at the surface where the strongest interaction between $\mathbf{E}_p$ and BNDC is expected. The highly n-doped area with dimensions $w_a \times h_a$ is highlighted by red color in the Fig. 2. The initial donor concentration N_D^+ was chosen accordingly to the criterion (5) and the device stability was investigated upon the results of the TDD calculations using (4) on the domain Ω marked in the Fig. 2. The heat dissipation is provided at the ground plane interface with boundary heat transfer coefficient htc, which completely substitute the real heat-sink in the simulations. Its value for the typical metal plate heat-sink should be in the range $10^4 \div 10^5$ Wm^{2}K^{-1} [10].

Using the parametric analysis we found that the best stable amplification performance of the ACPW were achieved for the active area dimensions $w_a = 320$ µm and $h_a = 60$ µm, heat transfer coefficient $htc = 10^5$ Wm^{2}K^{-1}, doping concentration $N_D^+ = 2\times10^{19}$ m^{-3} and bias voltage $V_a = 70$ V with resultant device temperature $T = 411$ K.

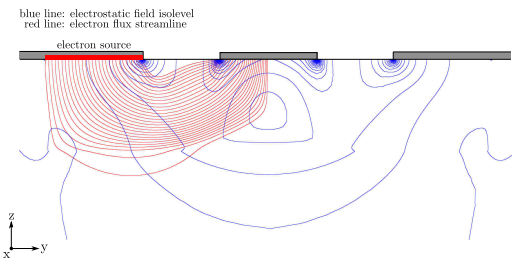

Figure 3. Effect of the electron flux repulsion from the surface caused by high intensity electric field at the metal edges

The solution of the TDD calculation at positive bias 50V applied at the central strip is depicted in the Fig. 3, where we visualize 30 stream lines of the electron flux placed equidistantly at the cathode with the length of the high doped area interface (source of electrons). The electrostatic field is presented by contour lines of equidistant values. We can observe the effect of the carrier dispersion in the substrate while the electrons are accelerated in –z axis direction by the high electric field values at the strip edges and pushed away from the surface into the substrate. As a result the electrons are spatially dispersed and flow out of the active area. Further more, the current density vector and the transversal components of the propagation wave are no longer parallel to each other. It means that, both assumptions of the effective interaction are not respected.

On the other hand, the effect at the voltage terminal edges can be exploited to enhance the interaction efficiency. If we consider the current flow perpendicularly respective to the terminal surface along entire length between voltage terminals (in parallel to z axis), and we take into account that areas of high electric field exhibits by considerably lower mobility, the high intensity electric field at the strip edges should focus the electron flux into a narrow beam. Such effect can be realized in the microstrip line configuration.

For this purpose we have developed the cross-section model of the 50 Ω active microstrip line (AML) on the low n-doped GaAs substrate with thickness of 100 µm according to the Fig. 4. The device stability was evaluated on the active domain, depicted by red color in the Fig. 4, using (4).

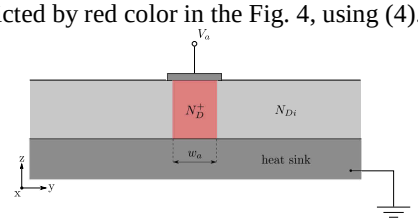

Figure 4. Active microstrip line structure.

We found that the best stable amplification performance of the AML were achieved for the active area width $w_a = 30$ µm, $htc = 10^5$ Wm^{2}K^{-1}, doping concentration $N_D^+ = 2\times10^{19}$ m^{-3} and bias voltage $V_a = 55$ V with resultant device temperature $T = 326$ K.

The solution of the TDD calculation at positive bias 50V applied at the strip is depicted in the Fig. 5. It is obvious that the high field effect at the strip edges affect significantly the path of the current flow by desired manner. The electron current density is focused under the strip to the narrower area and its vectors are in parallel to the transversal components of the fundamental mode. It follows that both assumptions of the effective interaction are met. Furthermore, the efficient heat dissipation is provided by close contact of the active area with the heat-sink interface at the ground plane.

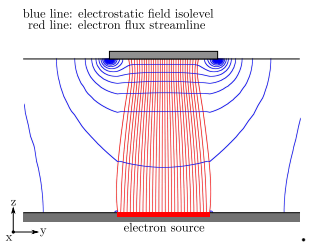

Figure 5. Focusing effect of the electron flux due to the high intensity electric field at the strip edges.

IV. Comparisons

If we consider the passive design of presented transmission lines, e.g. made on the semi-insulating GaAs substrate, we can found that the attenuation constants due ohmic losses in metallic parts considerably differ to each other. Therefore it is desirable to calculate the difference of the attenuation and phase constants between passive and active versions of the transmission lines. This way, we can clearly compare the effect of the active substrate on the transmission properties.

The calculation results of the attenuation constant difference $\Delta\alpha$ are depicted in the Fig. 6. for both devices. The magnitude of the negative values indicates the additional gain and the positive one the additional losses of the active design contrary to passive one. The better performance of the microstrip line is evident. The gain at 1 GHz is approximately the same for both devices with the value about 37 dBm^{-1}. In case of the ACPW, the gain decreases rapidly with the frequency to the value $\Delta\alpha = 0$ at $f \doteq 14$ GHz. The AML exhibits by more uniform gain characteristic and falls to value $\Delta\alpha = 0$ at the frequency $f \doteq 70$ GHz.

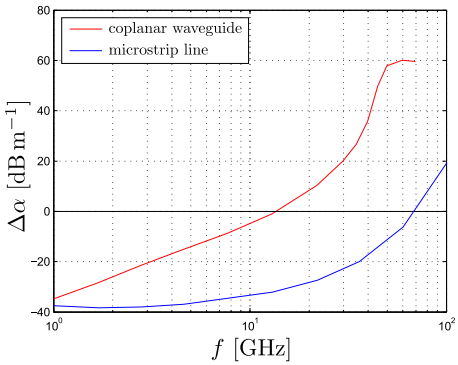

Figure 6. Frequency characteristic of the attenuation constant difference between passive and active transmission lines.

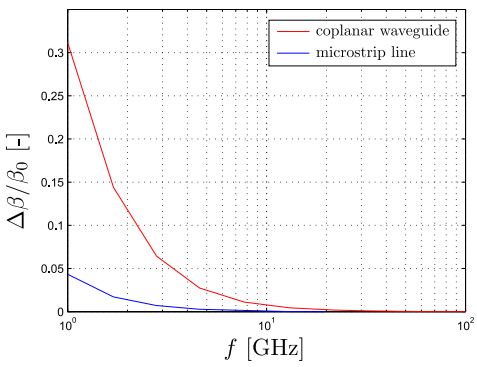

Figure 7. Frequency characteristic of the phase constant difference between passive and active transmission lines.

The calculation results of the phase constant difference $\Delta\beta$ are depicted in the Fig. 7. for both devices in the relative scale to the free space phase constant β_0. It is obvious that the AML contrary to the ACPW exhibits by lower relative phase shift about one order.

V. Conclusions

In this paper, the modeling issues of the distributed BNDC devices were discussed and the complex calculations of the active transmission lines up to 100 GHz are presented. The issue of the device stability and heat dissipation is also included in the device analysis. We have investigated the convectional concept based on the coplanar waveguide [1] and propose the more efficient solution based on the vertical configuration of voltage terminals. That way, we can focus the carrier flux into the narrow area and enhance the amplification efficiency of the device. This approach is demonstrated in the novel design of the active microstrip line.

Acknowledgment

Research described in this contribution was financially supported by the Czech Science Foundation under the grants no. 102/07/0688 and 102/08/H018. The research is a part of the COST project IC0603 financed by the grant of the Czech Ministry of Education no. OC08027 and the research centre LC06071.

References

[1] P. L. Fleming, "The active medium propagation device," *Proceedings of the IEEE*, vol. 63, no. 8, pp. 1253-1254, August 1975.

[2] D. V. Lioubtchenko, S. Tretyakov, S. Dudorov, "Millimeter-Wave Waveguides," *Boston: Kluwer Academic Publishers*, 2003.

[3] M. Zhang, C. Wu, K. Wu, J. Litva, "Losses in GaAs microstrip and coplanar waveguide," *Proceedings of Microwave Symposium Digest*, vol.2, pp. 971 - 974, June 1992.

[4] A. Jelenski, I. E. Tralle, V. A. Sizyuk, "Simulation of a Gallium Arsenide Running Wave Amplifier with a Schottky Barrier by the Monte Carlo Method," *Journal of Engineering and Thermophysics*, vol. 71, no. 5, pp. 878-885, 1998.

[5] G. Wang, R. W. Dutton, C. S. Rafferty, "Device-level simulation of wave propagation along metal-insulator-semiconductor interconnects," *IEEE Transaction on Microwave Theory and Techniques*, vol. 50, no. 4, pp. 1127-1136, April 2002.

[6] S. Selberherr, "Analysis and Simulation of Semiconductor Devices," *Hiedelberg: Springer-Verlag*, 1984.

[7] –,"DESSIS," *Zurich: ISE Integrated Systems Engineering AG*, 2004.

[8] M. Shur, "GaAs Devices and Circuits," *Springer, London - New York*, 1987.

[9] D. H. Rees, "Hot Electron Effect at Microwave Frequencies in GaAs," *Solid State Communications*, vol. 7, pp. 267-269, 1969.

[10] M. Pokorný, "Modeling of Microwave Semiconductor Structures," *Brno: Brno University of Technology, The Faculty of Electrical Engineering and Communication*, Doctoral thesis, 2011.